AIIM

Association for Information and Image Management

1100 Wayne Avenue, Suite 1100
Silver Spring, Maryland 20910

301/587-8202

Centimeter

1 2 3 4 5 6 7 8 9 10 11 12 13 14 15 mm

1 2 3 4 5

Inches

MANUFACTURED TO AIIM STANDARDS
BY APPLIED IMAGE, INC.

1 of 1

LBL-35510
UC-410

OPTIMIZATION DESIGN STUDY FOR AN ELLIPTICAL WIGGLER AT THE ADVANCED LIGHT SOURCE

Steve Marks, Wayne McKinney, Howard Padmore and Anthony Young

Advanced Light Source
Accelerator and Fusion Research Division
Lawrence Berkeley Laboratory
University of California
Berkeley,CA 94720

July 15, 1994

*This work was supported by the Director, Office of Energy Research, Office of Basic Energy Sciences, Materials Sciences Division of the U.S. Department of Energy, under Contract no. DE-AC03-76SF00098

Optimization Design Study for an Elliptical Wiggler at the Advanced Light Source

S. Marks, W. McKinney, H. Padmore, A. Young

Advanced Light Source, Lawrence Berkeley Laboratory, University of California, Berkeley, California 94720

Abstract

This paper describes a design study with the objective of optimizing spectral performance of an elliptical wiggler to be installed at the Lawrence Berkeley Laboratory Advanced Light Source (ALS). This device is to produce circularly polarized radiation in the energy range of 50 eV to 10 KeV. A figure of merit, which is a function of flux density and degree of circular polarization, is introduced as the objective function for optimization. An optimum set point for a particular photon energy is characterized by values of peak vertical field, horizontal deflection parameter, and vertical aperture. Optimum performance is evaluated for the nominal ALS operating energy of 1.5 GeV.

I. Introduction

Circularly polarized x-rays have become an important tool in the study of the spin state of magnetically ordered materials. Circularly polarized x-rays can be produced by the conversion of linearly polarized radiation using phase plates of various varieties,[1,2] but these methods often either suffer from low efficiency or impose unwanted constraints on tunability or energy resolution. Circularly polarized radiation can be produced by observation of bending magnet radiation above and below the orbit plane, and this technique has been extensively used from the VUV to the x-ray spectral range. This method suffers from two disadvantages. First, the intensity decreases off-axis, and for many experiments a small circular dichroism requires maximum photon flux. Secondly, right and left circularly polarized components are in angularly separated beams, and small differences in the properties of the optical system that the beam intersects are reflected as noise in the dichroism signal. These problems can be overcome by an elliptical wiggler.[3] The circularly polarized light which normally occurs above and below the orbit plane is made to emerge along the optical axis of the device by appropriate deflection of the beam in the vertical direction. The vertical orbit is modulated with the same periodicity as the horizontal orbit but shifted by 1/4 period. Thus the vertical angle as the particle passes successive vertical poles of opposite magnetic polarity is reversed, and circularly polarized radiation of the same helicity is emitted from each pole along the axis of the device. A device of this type with permanent magnet vertical and horizontal wigglers was reported by Yamamoto, et. al.[4] Change of helicity in this case can only be accomplished by longitudinal translation of the magnetic array, and hence is slow.

The elliptical wiggler being constructed at the Advanced Light Source (ALS) is similar to that at the Photon Factory,[4] except that the vertical field is produced by a variable gap hybrid permanent magnetic structure and the horizontal field is produced by electromagnets. This allows the rapid reversal of the horizontal field by reversing the coil current. The maximum modulation frequency is limited by eddy currents in the vacuum chamber and the adjacent magnetic material.

The ALS device is designed for a maximum frequency of at least 1 Hz. A more complete description of the device has been given by Hoyer, et. al.[5]

The spectral output of an elliptical wiggler involves a trade-off between flux density and degree of circular polarization. As the alternating vertical deflection resulting from the horizontal magnetic field is increased, the degree of circular polarization increases, but the on-axis flux density decreases. Therefore, optimization must consider some appropriate mix of the two quantities. The product of the square of the degree of circular polarization and the flux density is the appropriate figure of merit for experiments using single event counting to detect asymmetry between the effect of left and right circularly polarized radiation. We consider the integral of this merit function

$$M = \int_{\Delta\psi}\int_{\Delta\phi} P_c |P_c| \frac{d^2F}{d\phi d\psi} d\phi d\psi \tag{1}$$

where P_c is the degree of circular polarization, F is flux, and $\Delta\phi$ and $\Delta\psi$ are the horizontal and vertical apertures, respectively. Note that Eq. 1 is defined such that the sign associated with P_c is maintained.

A detailed design study has been conducted to evaluate and optimize the spectral performance of the elliptical wiggler for photon energies in the range 50 eV to 10 KeV and for storage ring energies of 1.5 GeV and 1.9 GeV.[6] This paper provides a summary of the procedure and results.

II. Theoretical Background

We treat the radiation as that from a series of bending magnets of alternating polarity. The bend magnet formulas assume that electrons follow a circular trajectory corresponding to a constant magnetic field.[7] We account for variation in vertical field and vertical deflection resulting from horizontal field by using local values of vertical field and vertical angle at each point along the electron trajectory to calculate spectral properties. The electric field components for the bend magnet case are

$$E_\sigma(\psi,\varepsilon) = \frac{\sqrt{3}}{2\pi}\gamma\frac{\varepsilon}{\varepsilon_c}(1+\chi^2)(-i)K_{2/3}(\eta) \tag{2}$$

$$E_\pi(\psi,\varepsilon) = \frac{\sqrt{3}}{2\pi}\gamma\frac{\varepsilon}{\varepsilon_c}(1+\chi^2)\frac{\chi}{\sqrt{1+\chi^2}}K_{1/3}(\eta) \tag{3}$$

The subscripts σ and π refer to the two components of linear polarization. The terms ε and ε_c are the photon energy and critical energy, respectively. The critical energy is defined as

$$\varepsilon_c[KeV] = 0.665E^2[GeV]B_p[T] \tag{4}$$

where E is the electron energy, and B_p is the peak magnetic field strength. The terms $K_{2/3}$ and $K_{1/3}$ in Eqs. 2 and 3 are modified Bessel functions. The terms χ and η are defined as

$$\chi = \gamma\psi, \quad \eta = \frac{1}{2}\frac{\varepsilon}{\varepsilon_c}(1+\chi^2)^{3/2} \tag{5}$$

where ψ is the vertical angle, and γ is the electron rest mass energy.

The two components of flux density are

$$\frac{d^2F_\sigma}{d\phi d\psi} = \frac{\Delta\varepsilon}{\varepsilon}E_\sigma^2 , \quad \frac{d^2F_\pi}{d\phi d\psi} = \frac{\Delta\varepsilon}{\varepsilon}E_\pi^2 \tag{6}$$

where $\Delta\varepsilon/\varepsilon$ is the fractional bandwidth.

The degree of circular polarization is the fraction of circularly polarized flux and is defined as the ratio of the Stokes parameters s_3 and s_0.[8]

$$P_c = \frac{s_3}{s_0}, \; s_0 = E_\sigma^2 + E_\pi^2 , \; s_3 = 2E_\sigma^* E_\pi \tag{7}$$

The term E_σ^* is the complex conjugate of the electric field component define in Eq. (2).

The vertical magnetic field is given by

$$B_y(z) = \sum_n B_{yn}\cos(nkz); \quad n = 1,3,5,... \tag{8}$$

where z is the coordinate along the wiggler axis. The horizontal trajectory angle ϕ as a function of z is

$$\phi(z) = \frac{e}{\gamma m_e c}\int_{-\infty}^{z} B_y(\varsigma)d\varsigma = \frac{0.934\lambda_w[cm]}{\gamma}\sum_n \frac{B_{yn}[T]}{n}\sin(nkz) \tag{9}$$

The term λ_w is the period length of the wiggler. Using Eqs. 8 and 9, we can determine $B_y(\phi)$; this in conjunction with Eqs. 2 through 7 determines the spectral dependence on ϕ.

The horizontal magnetic field is given by

$$B_x(z) = \sum_n B_{xn}\sin(nkz); \quad n = 1,3,5,... \tag{10}$$

The resulting vertical angle ψ is

$$\psi(z) = \frac{e}{\gamma m_e c}\int_{-\infty}^{z} B_x(\varsigma)d\varsigma = -\frac{0.934\lambda_w[cm]}{\gamma}\sum_n \frac{B_{xn}[T]}{n}\cos(nkz) \tag{11}$$

Spectral flux density and polarization, given by Eqs. 2 through 7, have an explicit dependence upon the vertical angle, ψ. At each point along the electron trajectory ψ can be calculated using Eqs. 10 and 11.

III. Calculations

A set of procedures and codes have been developed to calculate the merit function M as defined in Eq. 1, as well as total flux and integrated flux weighted degree of circular polarization defined as

$$\hat{P}_c = \frac{1}{F}\int_{\Delta\psi}\int_{\Delta\phi} P_c \frac{d^2F}{d\phi d\psi}d\phi d\psi \tag{12}$$

For a particular photon energy and setting of B_y and K_x, the value of $\Delta\psi$ is such that M, as defined in Eq. 1, is 80% of the maximum value for an infinite $\Delta\psi$; let us call this value M_∞. The optimum values of B_y and K_x minimize $\Delta\psi$ subject to this 80% condition; i.e., $M = 0.8M_\infty$. The value B_y corresponds to peak vertical field. The value K_x is the effective deflection parameter defined as

$$K_x = 0.934\lambda_w[cm]\sum_n \frac{B_{xn}[T]}{n} \tag{13}$$

The optimization process is greatly simplified by the fact that the effects of B_y and K_x are largely decoupled. The value of M_∞ and initial estimates of B_y and K_x can be determined from calculations that do not explicitly invoke the horizontal field. This is illustrated in Fig. 1, which shows a plot of the distribution of M' in vertical angle, ψ, where M' is defined as

$$M' = \int_{\Delta\phi} P_c |P_c| \frac{d^2F}{d\phi d\psi} d\phi \tag{14}$$

The plot is for 300 eV photon energy, for B_y = 1.2 T and for K_x = 0 and K_x = 1.2. Note that changing K_x does not change the shape, but simply shifts the distribution. The value of M_∞, and therefore M, can be determined by integrating M' for K_x = 0. The optimum value of K_x approximately corresponds to the location of peak M' for K_x = 0. Note that the value of B_y which minimizes $\Delta\psi$ is not necessarily the value which maximizes M_∞.

Fig. 1 shows the distribution of M' for a single pole. Note that for the K_x = 0 curve M' is anti-symmetric about ψ, i.e., $-M'$ is mirrored about $\psi = 0$. This distribution corresponds to all poles with positive B_y polarity. The distribution for the adjacent pole, and all negative polarity poles, is reversed. As K_x is increased the $+M'$ distribution for positive poles moves to the left, while that for negative poles moves to the right until they overlap. Fig. 2 shows the overlap of positive and negative poles for optimum B_y and K_x values at 300 eV photon energy. For this case $\Delta\psi = \pm 0.223$ mrad.

The procedure for calculating an optimum at a given photon energy is summarized as follows. First, calculate M' and $\int M' d\psi$ for a series of B_y with K_x = 0. This identifies the value of M_∞, and thus M. This step provides an initial value for B_y and an approximate value for K_x. Then determine optimum B_y and K_x which minimize $\Delta\psi$ for the fixed value of M determined in the first step. For a particular iteration, fix B_y and vary K_x. Start with the initial value of B_y obtained in the first step; then try values above and below this to verity that $\Delta\psi$ has been minimized. In addition to M, values of flux, F, and $\hat{P}_c$ are calculated at the optimum point.

IV. Results

Table I summarizes the results of optimization for 1.5 GeV electron energy. The table includes optimum values of B_y, K_x, and vertical half-aperture, $\Delta\psi/2$, and the values of M for a series of photon energies ε. The results are for a fixed horizontal aperture, $\Delta\phi$, of ± 2.5 mrad. The data in the table reveal several important trends. The optimum value of B_y increases as the photon energy increases, in order to drive the intensity distribution to higher energy. Note that the peak field is reached for a photon energy of 1 KeV. Optimum K_x decreases with increasing photon energy as the width of the individual σ and π polarized components decrease in angular width. Optimized M is reasonably constant up to 1500 eV, and decreases rapidly at high photon energy. The degree of circular polarization is limited at 50 eV photon energy due to the maximum achievable K_x. At high photon energies the degree of circular polarization is limited by the

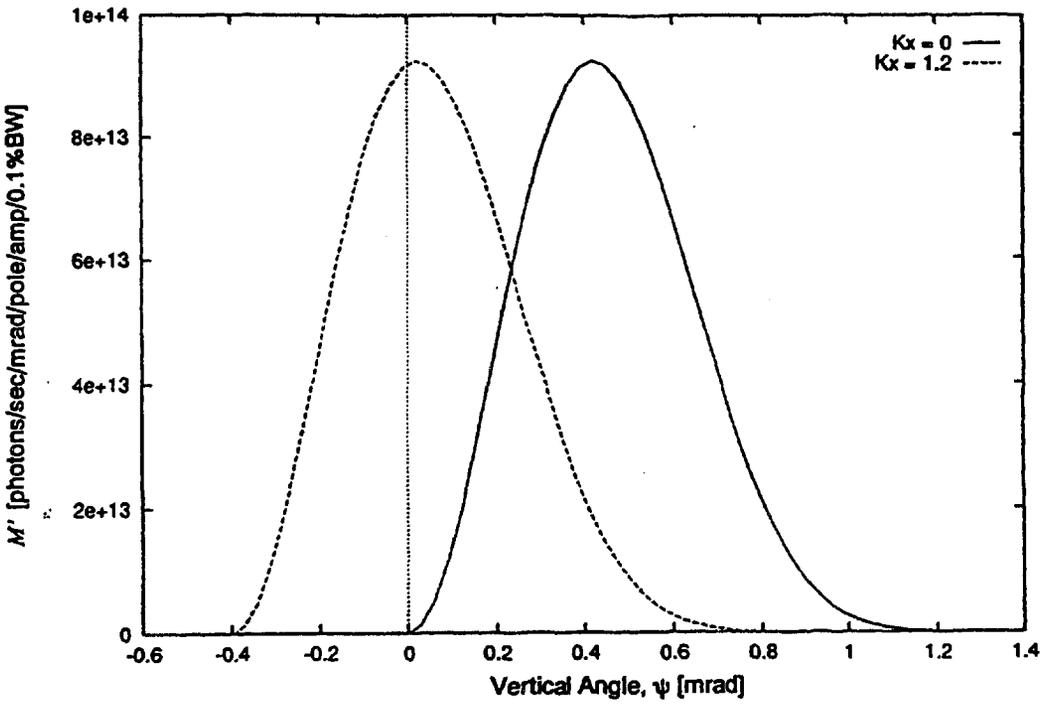

Figure 1: Plot of M' for 300 eV photon energy, 1.5 GeV electron energy, and B_y = 1.2 T.

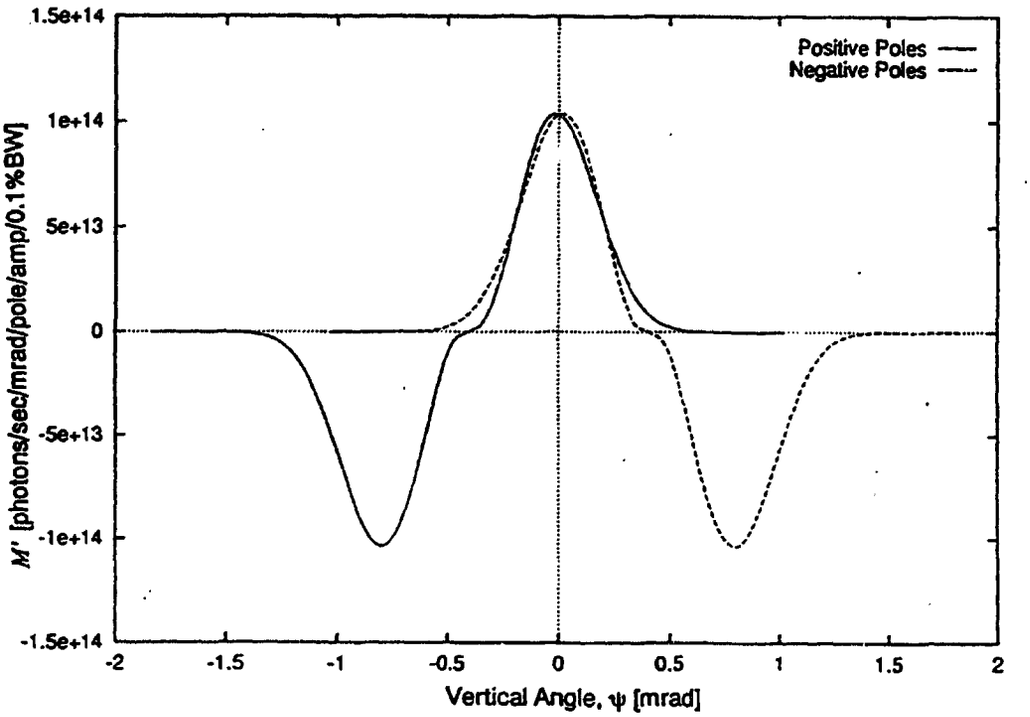

Figure 3: Optimum distribution of M' for 300 eV photon energy. For $M = 0.8M_{\infty}$, $\Delta\psi = \pm 0.223$ mrad.

reduced separation of σ and π components. At 1.9 GeV operation (maximum ALS energy) the performance at high photon energies will be greatly improved.

Table I Optimization for 1.5 GeV

ε eV	B_y Tesla	K_x	$\Delta\psi/2$ mrad	$M \times 10^{-13}$ photons/sec
50	0.4	1.5	0.333	3.49
100	0.5	1.49	0.256	3.65
150	0.5	1.30	0.229	3.65
300	0.8	1.13	0.220	3.66
700	1.6	1.07	0.212	3.59
1000	2.0	1.02	0.191	3.38
1500	2.0	0.88	0.165	2.94
3000	2.0	0.67	0.127	1.77
7000	2.0	0.48	0.091	0.415
10000	2.0	0.41	0.079	0.139

V. Summary

The information derived from the analysis summarized here provides a significant basis for optimizing the performance of the wiggler, and also in finding the optimum aperture required for the optical system. In addition, it provides a method to assess the sensitivity of the system to errors, such as noise in the horizontal field and power supplies, and to movement of the aperture.

In the analysis presented here, we have assumed that the optical depth of the device does not modify the polarization characteristics or the optimization. In reality, the depth of field effect will be significant; an example of the way this may modify our analysis can be demonstrated by considering an optical system focusing the light to a slit. The effect of the slit will be to impose a longitudinal probability function on the wiggler emission; in the limit of a vanishingly small slit, only radiation emitted from the center of the device will be accepted. The optical properties of the device, combined with its polarization properties, are being studied using phase space techniques.[9]

VI. Acknowledgement

This work was supported by the Director, Office of Energy Research, Office of Basic Energy Sciences, Materials Sciences Division of the U. S. Department of Energy, under Contract No. DE-AC03-76SF00098.

VII. References

1. P. Skalicky and C. Malgrange, Acta Crystallogr. A28 (1972) 501.
2. M. Hart and A. R. Lang, Acta Crystallogr. 19 (1965) 73.
3. P. Elleaume, Rev. Sci. Instrum. 60 (7), July, 1989.
4. S. Yamamoto, T, Shioya, S. Sasaki, H. Kitamura, Rev. Sci. Instrum. 60 (7), July, 1989.
5. E. Hoyer, J. Akre, D. Humphries, S. Marks, Y. Minamihara, P. Pipersky, D. Plate, R. Schlueter, these proceedings.
6. S. Marks, LBL Report, ALS Beam Line Note 207 (June 1994).
7. K. J. Kim, *Physics of Particle Accelerators*, M. Month & M Dienes ed., AIP Conference Proceedings 184, vol. 1 (1989).
8. Born and Wolf, *Principles of Optics* (Pergamon, 1980).
9. G. E. van Dorseen, H. A. Padmore and W. Joho, SPIE Vol. 2013, San Diego, July 1993.

DATE
FILMED
10/5/94

END